Journal of Chemical Crystallography (2018) 48:131–137
https://doi.org/10.1007/s10870-018-0720-8

ORIGINAL PAPER

Crystallographic and Computational Studies of Non-Covalent Interactions of Molecular Clips with a Series of Small Solvent Molecules

Madhubabu Alaparthi[1] · Dayton Jonathan Vogel[1] · Andrew G. Sykes[1]

Received: 9 February 2018 / Accepted: 14 July 2018 / Published online: 17 July 2018

Abstract

Molecular clips hold the potential of self-association and the ability to form host–guest complexes. Here we describe the synthesis of a 1,2-dimethoxyphenyl terminated glycoluril molecular clip (**2**) that binds with smaller solvent molecules by π···H–C and C=O···H–O non-covalent interactions. We obtained single crystals of **2** and **2** + CH_2Cl_2, CH_3OH, CH_3CN, and DMF solvents complexed within the clip. These solvents always form two π···H–C interactions between the aromatic rings in the clip, and CH_3OH formed an additional C=O···H–O hydrogen bond with the glycoluril carbonyl group. Based on single crystal data we found that π···H–C interactions of **2** + CH_2Cl_2 are stronger than **2** + CH_3CN and **2** + DMF, due to the presence of stronger electron withdrawing groups in CH_2Cl_2, which lead to a decrease in dihedral angle of two glycoluril aromatic planes. We also investigated the non-covalent interaction energies of these solvent molecules with **2** using computational methods.

Graphical Abstract

Several solvent adducts of a glycoluril derivative have been isolated and characterized by single crystal X-ray diffraction, revealing two common pi···H–C non-covalent bonds within the molecular clip.

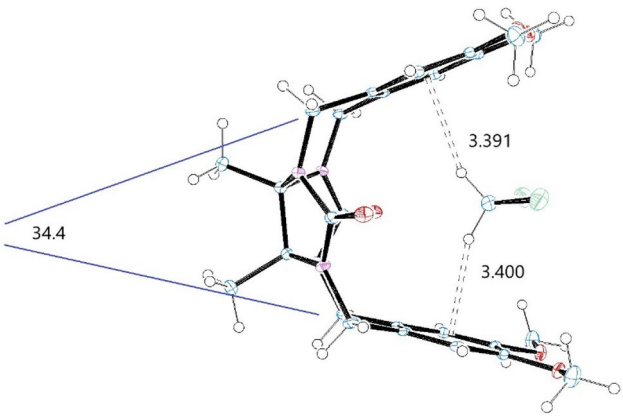

Keywords Molecular clip · Crystallography · Calculation · Solvent complexes · Glycoluril

Introduction

In 1905, Behrend first introduced glycoluril building blocks [1], followed by the synthesis of substituted glycolurils by Biltz in 1907 [2], which have recently been reviewed [3, 4]. Clark first reported the X-ray crystal structure of the

Electronic supplementary material The online version of this article (https://doi.org/10.1007/s10870-018-0720-8) contains supplementary material, which is available to authorized users.

✉ Andrew G. Sykes
asykes@usd.edu

Extended author information available on the last page of the article

unsubstituted glycoluril [5], a molecule with relatively high symmetry and a closely related structure to that of urea. The structures of numerous substituted glucolurils have also been reported, all showing bent backbones that form the clip motif [6–9]. Over the past three decades, molecular recognition chemistry has increased in popularity with applications ranging from host–guest chemistry, catalysis, supramolecular and biomedical applications [10–14]. Hexameric cyclic cucurbiturils (multiple linked glycoluril units) were reported by Freeman and Williams, exhibiting a ~ 5.5 Å diameter cavity within the macrocyclic structure [15, 16]. Cyclic cucurbiturils are named by indicating the number of glycoluril building blocks involved, such as CB[5] to CB[8] [17]. The cavity size of larger CB molecules enables them to form 1:1 binary complexes [18, 19] and even 1:1:1 heteroternary complexes [20, 21]. The catalytic properties of cyclic cucurbiturils were later investigated where the internal cavity helped in securing kinetic acceleration of cycloaddition reactions (ca. 10^5-fold) [22]. A number of unique one-dimensional coordination polymers have been produced by reacting *N*,*N*-bis(4pyridylmethyl)-1,4-diaminobutane, CB[6] and various metal ions to get threaded molecular necklaces [23–25]. Rebek et al. has reported dimeric glycoluril capsules, the famous tennis ball structure, where reversible encapsulation of Xenon was found in a self-assembled dimer [26], and the self-assembly of methylene bridged glycoluril dimers appended with carboxylic groups produced hydrophobic interiors [27]. Nolte has also investigated self-assembled, functional nanometer-sized architectures of bilayer vesicular aggregates of aza-crown functionalized CB units [28, 29]. Most recently, Isaacs has reported water soluble CB macrocycles [30], assisted dissociation activity of CB[7] with bovine carbonic anhydrase [31], and the synthesis of acyclic cucurbituril molecular containers that enhance the solubility and bioactivity of poorly soluble pharmaceuticals [32, 33]. Here we report the synthesis of a simple glycoluril derivative and the resulting association with a series of solvent molecules via non-covalent interactions within the molecular cleft.

Experimental

General

The synthesis of the 3,7-methylglucoluril-2,4,6,8 cyclic ether (Compound **1**) starting material has previously been reported [4]. ^{1}H- and ^{13}C-NMR spectra were recorded using a Bruker 400 MHz spectrometer at room temperature in $CDCl_3$ and are presented in the supplemental material.

Synthesis

2 was synthesized using a very similar procedure that was previously reported for the 1,4-dimethoxy isomer [30], and the characterization data matches the proposed structure in Scheme 1. The ^{1}H NMR signal at δ6.76 (s, 4H) is due to the aromatic hydrogen atoms; δ4.58 (d, J = 15.2 Hz, 4H) and δ0.29 (d, J = 15.8, 4H) are due to the inequivalent hydrogen atoms from the methylene bridging protons; δ3.82(s, 12H) are from the 12 methoxy protons, and δ1.73 (s, 6H) is from the six methyl protons, which supports **2** formation (Figure S1). Further investigation by ^{13}C NMR showed δ156.0 for the carbonyl group of the glycoluril, δ147.5, δ129.8, δ113.2, are due to the aromatic carbon atoms, δ55.9 for the $-OCH_3$ groups, δ43.6 from the bridging CH_2 groups, and δ16.8 due to the methyl protons which also supports **2** formation (Figure S2). A DEPT-135 experiment was conducted to determine unequivically the CH_2 signal, which was found inverted at δ43.6 in the spectrum (Figure S3).

Crystallography

X-ray single-crystal diffraction data were collected using MoKα radiation (λ = 0.71073 Å) on a Bruker CCD APEXII diffractometer at 100 K. Structures were solved by direct methods using SHELXL-97 in conjunction with standard difference Fourier techniques and subsequently refined by full matrix least-square analyses. All hydrogen atoms were placed in ideal positions except the methanol proton in the

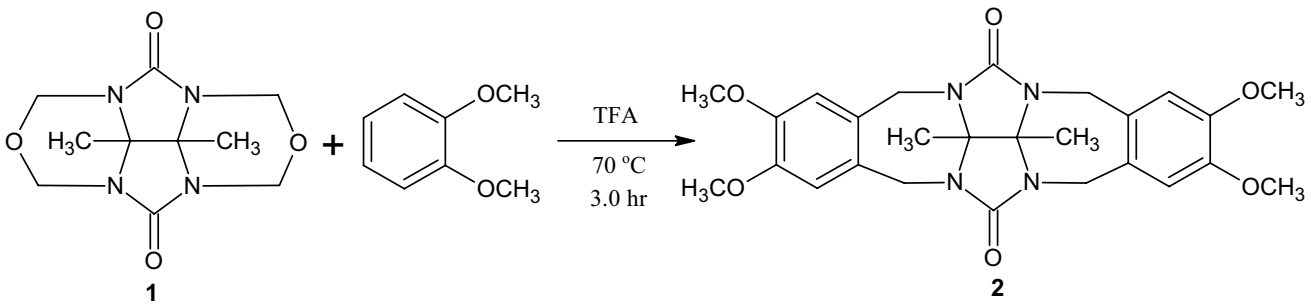

Scheme 1 Reaction scheme of **2**

structure of CB1 + MeOH, and all non-hydrogen atoms were refined anisotropically. The DMF solvent in the **2** + DMF structure is disordered over two positions in the same plane in a 16:84 ratio, and the smaller occupancy was kept isotropic. Detailed crystal structure information is listed in Table S1.

Computation

A first qualitative picture of various guest host molecule interaction energies are provided using the MP2/LANL2DZ level of theory. To compute an interaction energy, E_{int}, the guest host complex, E_{AB}, is separated into individual components, E_A and E_B, with binding energy calculated through

$$E_{\text{int}} = E_{AB} - E_A - E_B \quad (1)$$

The total energies are calculated through single point SCF calculations for each of the five systems. The atomic coordinates are imported from experimentally determined XRD data, providing exact orientation of the guest host complex.

The use of Eq. 1 provides an initial trend in how each guest molecule interacts with the host molecule. However, the interaction type under consideration, non-covalent interaction, requires a more thorough investigation. Correction for the weak chemical interaction has been addressed previously, most specifically through implementation of BSSE corrections to the interaction energies [34–36]. The BSSE provides a correction to weak interactions due to basis set overlap between the guest and host complex. The BSSE corrected interaction energies have been calculated through previously published methods [37].

Interaction energies for each of the four systems have been calculated from electronic structure calculations in Gaussian 09 software [38]. Calculated energies were computed using DFT (B3LYP [39–42]/6-311G [43], B3LYP/6-311G** [44], ωB97XD [45]/6-311G, and ωB97XD/LANL2DZ [46, 47]) and MP2 [48] (6-311G and LANL2DZ), Fig. 1.

Results and Discussion

Crystallography

We successfully obtained X-ray quality crystals of compounds **2**, **2** + CH_3OH, **2** + CH_2Cl_2, **2** + CH_3CN, and **2** + DMF. Crystals were grown by slowly diffusing diethyl ether into a CH_2Cl_2/CH_3OH (10%) mixture for **2** + CH_2Cl_2 crystals, CH_3OH/DMF (50%) for **2** + DMF crystals, CH_3CN/CH_3OH (10%) for **2** + CH_3CN crystals, and CH_3OH (100%) for **2** + CH_3OH crystals. **C**rystals of **2** containing no solvent were grown by diffusion of ethyl ether into a DMF-ethyl acetate mixture. Crystallographic and refinement data

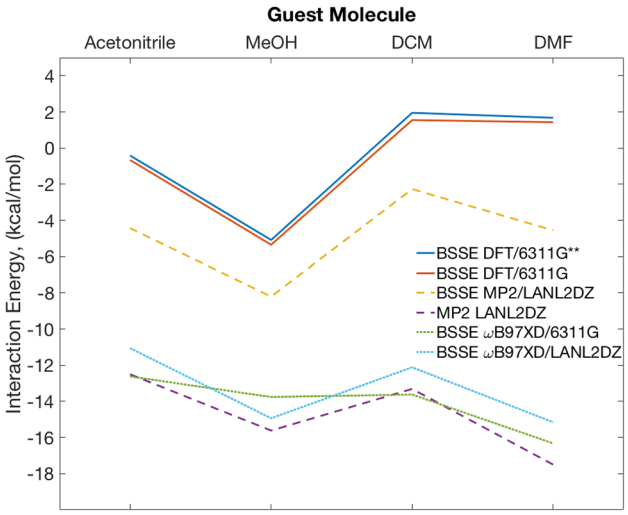

Fig. 1 Calculated guest–host interaction energies for **2** with four guest molecules: acetonitrile, methanol (MeOH), dichloromethane (DCM), and dimethylformamide (DMF). Energies are calculated for DFT at B3LYP (solid lines), MP2 (large dashes), and DFT ωB97XD (small dashes) levels of theory with and without a BSSE correction, as highlighted

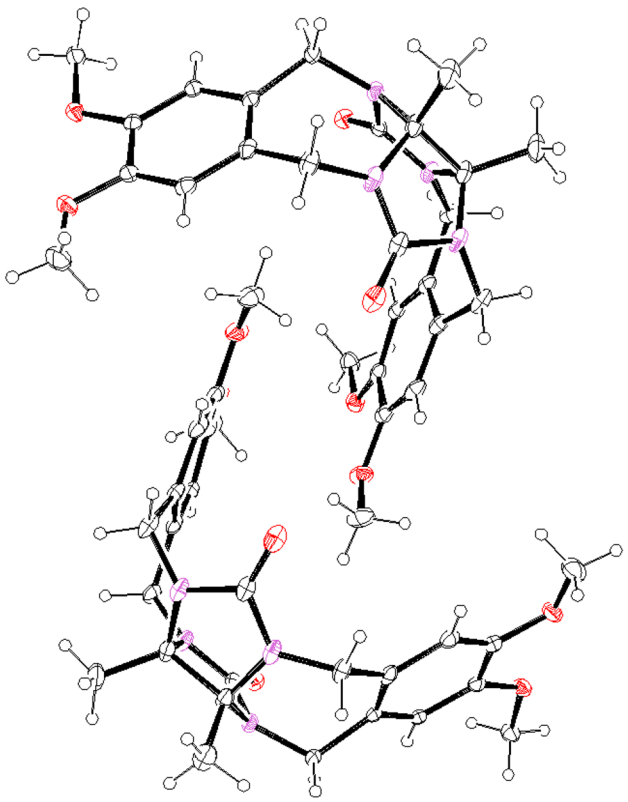

Fig. 2 Crystal structure of **2** with no solvent present, exhibiting interpenetration of a neighboring glucoluril molecule

are listed in Table S1. The crystal structure of **2** (Fig. 2), without solvent present, has slightly interpenetrating methoxy groups of neighboring CB molecules that produces a large dihedral angle between the two aromatic planes of 47.0° and 46.7° (Fig. 3a, two molecules in the asymmetric unit). The single closest π···H–C distance in this structure is a lengthy ~ 4.3 Å however, with most π···H–C distances over 4.5 Å (as measured in all cases from the centroid of the aromatic ring to the solvent carbon heavy atom). The **2** + CH_3CN crystal structure shows two intermolecular, T-shaped π···H–C donor–acceptor bonds measured as 3.417 Å (C27—(C8–C13) PLANE) and 3.554 Å

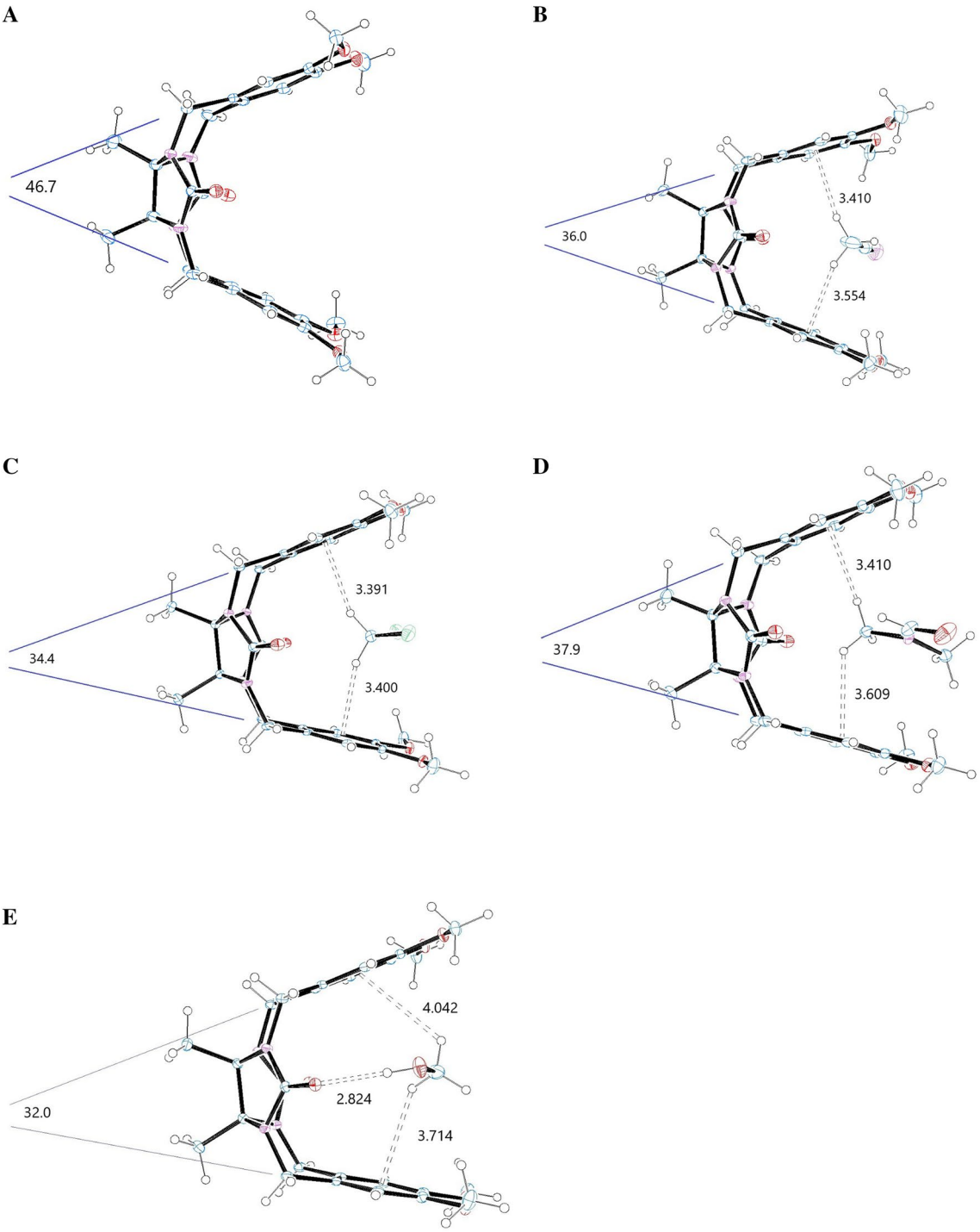

Fig. 3 Crystal structures of **a 2, b 2** + CH_3CN, **c 2** + CH_2Cl_2, **d 2** + DMF, **e 2** + CH_3OH showing dihedral angles between the aromatic planes, the π···H–C intermolecular distances, and one O–H···O hydrogen bond in E

(C27—(C18–C23) PLANE) and a much smaller dihedral angle between the two aromatic rings of 36.0° results (Fig. 3b). We observed a small decrease in the dihedral angle when two similar intermolecular π···H–C bonds are formed with CH_2Cl_2 in the **2** + CH_2Cl_2 crystal structure (Fig. 3c). The π···H–C distance are 3.391 Å (C27—(C8–C13) PLANE) and 3.400 Å (C27—(C18–C23) PLANE) with a dihedral angle between the two aromatic rings measured as 34.4°. Immobilizing DMF within the molecular clip, the two intermolecular π···H–C bond distances are slightly longer 3.609 Å (C1OO—(C19–C24) PLANE) and 3.410 Å (C1OO—(C9–C14) PLANE) and results in a net increase in the dihedral angle between the two aromatic rings measured as 37.9° (Fig. 3d). Methanol, the last solvent to be isolated within the molecular clip, also forms two long π···H–C non-covalent interactions (3.714 and 4.042 Å) and an additional classic hydrogen bond (C=O···HO–CH_3 = 2.824 Å) is also formed between the glycoluril carbonyl oxygen and the methanol OH group (Fig. 3e). In almost all cases, the solvent hydrogen atoms are centered above the middle of the aromatic rings located on the glucoluril. Exceptions to this are in A where the methoxy groups do no completely penetrate into the neighboring glucoluril and one particularly long π···H–C interaction for the MeOH adduct which is not centered above the aromatic ring.

Computational Investigation

To further enhance the understanding of the crystallographic data, computational methods were utilized to study guest host interaction energies. In this study, the system is comprised of a host and guest molecule represented by glycoluril and solvent molecules, respectively. The interaction energies of guest solvent molecules are of interest for multiple reasons, the first being an overall application of the host system as a solvent trap or delivery system, and a second is to promote or hinder formation of larger supramolecular systems comprised of individual glycoluril molecules.

To study the level of guest–host interaction, non-covalent interaction energies for T-shaped π···H–C and CO···H–O hydrogen bonds were studied using Gaussian09 software with varying methods and functionals. Total energies for the guest and host were calculated as individual pieces as well as the total complex. To find the interaction energy the total energies were used in $E_{int} = E_{tot} - (E_h + E_g)$, where E_{int}, E_{tot}, E_h, and Eg correspond to the energy of interaction, total, host, and guest, respectively. The total energies for each calculation were performed as single point energy calculations as all geometries were taken from crystallographic data. The electron density distribution electrostatic potential (ESP) maps, Figure S4, are plotted over atomistic models. The ESP maps provide the localized charge following single point electronic structure calculations. The color coding for the charge distribution shows positive charge as red and negative charge as blue.

Initial interaction energies provided were calculated at the MP2/LANL2DZ level of theory. For direct comparison, the BSSE correction has been applied to the four complexes and recalculated to highlight the energy shift at the MP2/LANL2DZ level of theory. The relative energy trend between guest molecules is maintained with and without the BSSE correction, but the calculated interaction energy is shifted.

Interaction energies calculated with BSSE corrected DFT B3LYP are nearly identical, as the change in calculation is a small increase in basis set. The near identical interaction energies found through BSSE corrected DFT are to be expected as there is only an increase in basis size. An increase of basis size is known to reduce the need for BSSE corrections, and the comparison shows the relative stability of the BSSE correction values [49]. The trend in interaction energies of the DFT B3LYP calculations also show the same relative trending between guest molecules found using the MP2 level of theory. Previously calculated test structures have found that pi-H bonding in bromobenzene molecules is found to be − 11.9 kcal/mol [50]. The dispersion corrected ωB97XD interaction energies show similar energies, but are unique chemical systems. The interaction energy value is highly dependent on the interacting molecules and have been shown to range greatly [51, 52].

Methanol produces the complex with the smallest dihedral angle between the two aromatic planes, and is consistent with the strongest interaction energy calculated, almost certainly due to the added hydrogen bond to the CB unit being present. Excluding the MeOH complex, the DMF complex has the largest dihedral angle of all the complexes which decreases in magnitude as the bulky substituents reduce in size, DMF > CH_3CN > CH_2Cl_2, These three complexes exhibit relatively comparable interaction energies.

Conclusion

A simple molecular cleft has been synthesized and readily forms adducts with solvent molecules. With support from single-crystal XRD and computational data, we have demonstrated that bis(1,2-dimethoxyphenyl)glucoluril (**2**) forms two intermolecular π···H–C non-covalent bonds with small solvent molecules. These favorable interactions dramatically reduce the dihedral angles for the solvent adducts of **2**, as compared to the solvent free parent. Otherwise, no clear trend in the dihedral angle between the two aromatic rings is apparent due to either π···H–C bond distances as observed or the interaction energies as calculated, with the exception of the MeOH adduct which has an additional C=O···H–O hydrogen bond, the most favorable interaction energy, and the smallest dihedral angle observed. Interactions related

to packing forces within the unit cell were not addressed in this study.

Acknowledgements The authors thank NSF-EPSCOR (EPS-0554609) and the South Dakota Governor's 2010 Initiative for financial support and the purchase of a Bruker SMART APEX II CCD diffractometer. The 400 MHz NMR was provided by funding from NSF-CHE-1229035.

References

1. Behrend R, Meyer E, Rusche FI (1905) Ueber condensationsproducte aus glycoluril und formaldehyd. Eur J Org Chem 339(1):1–37
2. Biltz H (1907) Zur Kenntnis der Glyoxalone. Chem Ber 40(4):4799–4806
3. Petersen H (1973) Syntheses of cyclic ureas by α-ureidoalkylation. Synthesis 5:243–292
4. Jansen K, Wego A, Buschmann H-J, Schollmeyer E, Döpp D (2003) Glycoluril derivatives as precursors in the preparation of substituted cucurbit [n] urils. Des Monomers Polym 6(1):43–55
5. Xu S, Gantzel PK, Clark LB (1994) Glycoluril. Acta Cryst 50(12):1988–1989
6. Himes V, Hubbard C, Mighell A, Fatiadi A (1978) 3a, 6a-Dimethylglycoluril {3a,6a-dihydro-3a,6a-dimethylimidazo [4, 5-d] imidazole-2,5 (1H,6H)-dione}. Acta Cryst 34(10):3102–3104
7. Boileau J, Wimmer E, Gilardi R, Stinecipher M, Gallo R, Pierrot M (1988) Structure of 1,4-dinitroglycoluril. Acta Cryst 44(4):696–699
8. Dekaprilevich M, Suvorova L, Khmelnitskii L (1994) 1,6-Dimethyltetrahydroimidazo [4,5-d]-imidazole-2,5(1H, 6H)-dione monohydrate. Acta Cryst 50(12):2056–2058
9. Sun S, Britten JF, Cow CN, Matta CF, Harrison PH (1998) The crystal structure of 3,4,7,8-tetramethylglycoluril. Can J Chem 76(3):301–306
10. Assaf KI, Nau WM (2015) Cucurbiturils: from synthesis to high-affinity binding and catalysis. Chem Soc Rev 44(2):394–418
11. Pemberton BC, Raghunathan R, Volla S, Sivaguru J (2012) From containers to catalysts: supramolecular catalysis within cucurbiturils. Chem Eur J 18(39):12178–12190
12. Loh XJ (2014) Supramolecular host–guest polymeric materials for biomedical applications. Mater Horiz 1(2):185–195
13. Masson E, Ling X, Joseph R, Kyeremeh-Mensah L, Lu X (2012) Cucurbituril chemistry: a tale of supramolecular success. RSC Adv 2(4):1213–1247
14. Zhang J, Ma PX (2010) Host–guest interactions mediated nanoassemblies using cyclodextrin-containing hydrophilic polymers and their biomedical applications. Nano Today 5(4):337–350
15. Freeman W, Mock W, Shih N, Cucurbituril (1981) Cucurbituril. J Am Chem Soc 103(24):7367–7368
16. Mock WL, Manimaran T, Freeman WA, Kuksuk RM, Maggio JE, Williams DH (1985) A novel hexacyclic ring system from glycoluril. J Org Chem 50(1):60–62
17. Barrow SJ, Kasera S, Rowland MJ, del Barrio J, Scherman OA (2015) Cucurbituril-based molecular recognition. Chem Rev 115(22):12320–12406
18. Zhao N, Lloyd GO, Scherman OA (2012) Monofunctionalised cucurbit [6] uril synthesis using imidazolium host–guest complexation. Chem Commun 48(25):3070–3072
19. Mock W, Irra T, Wepsiec J, Manimaran T (1983) Cycloaddition induced by cucurbituril: a case of Pauling principle catalysis. J Org Chem 48(20):3619–3620
20. Olga A, Samsonenko DG, Fedin VP (2002) Supramolecular chemistry of cucurbiturils. Russ Chem Rev 71(9):741–760
21. Saadeh H, Wang LM, Yu LP (2000) Supramolecular solid-state assemblies exhibiting electrooptic effects. J Am Chem Soc 122:546–547
22. Mock WL, Irra TA, Wepsiec JP, Adhya M (1989) Catalysis by cucurbituril. The significance of bound-substrate destabilization for induced triazole formation. J Org Chem 54(22):5302–5308
23. Whang D, Kim K (1997) Helical polyrotaxane: cucurbituril 'beads' threaded onto a helical one-dimensional coordination polymer. Chem Commun 24:2361–2362
24. Whang D, Park K-M, Heo J, Ashton P, Kim K (1998) Molecular necklace: quantitative self-assembly of a cyclic oligorotaxane from nine molecules. J Am Chem Soc 120(19):4899–4900
25. Roh SG, Park KM, Park GJ, Sakamoto S, Yamaguchi K, Kim K (1999) Synthesis of a five-membered molecular necklace: a 2 + 2 approach. Angew Chem Int Ed 38(5):637–641
26. Branda N, Grotzfeld RM, Valdes C, Rebek J (1995) Control of self-assembly and reversible encapsulation of xenon in a self-assembling dimer by acid-base chemistry. J Am Chem Soc 117(1):85–88
27. Isaacs L, Witt D, Lagona J (2001) Self-association of facially amphiphilic methylene bridged glycoluril dimers. Org Lett 3(20):3221–3224
28. Rowan AE, Elemans JA, Nolte RJ (1999) Molecular and supramolecular objects from glycoluril. Acc Chem Res 32(12):995–1006
29. Elemans JA, Rowan AE, Nolte RJ (2000) Self-assembled architectures from glycoluril. Ind Eng Chem Res 39(10):3419–3428
30. Lagona J, Wagner BD, Isaacs L (2006) Molecular-recognition properties of a water-soluble cucurbit [6] uril analogue. J Org Chem 71(3):1181–1190
31. Ghosh S, Isaacs L (2010) Biological catalysis regulated by cucurbit [7] uril molecular containers. J Am Chem Soc 132(12):4445–4454
32. Wu A, Chakraborty A, Witt D, Lagona J, Damkaci F, Ofori MA, Chiles JK, Fettinger JC, Isaacs L (2002) Methylene-bridged glycoluril dimers: synthetic methods. J Org Chem 67(16):5817–5830
33. Ma D, Hettiarachchi G, Nguyen D, Zhang B, Wittenberg JB, Zavalij PY, Briken V, Isaacs L (2012) Acyclic cucurbit [n] uril molecular containers enhance the solubility and bioactivity of poorly soluble pharmaceuticals. Nat Chem 4(6):503–510
34. Boys SF, Bernardi F (1970) The calculation of small molecular interactions by the differences of separate total energies. Some procedures with reduced errors. Mol Phys 19:553–566
35. Handy NC, Comment (2002) Comment on "The Calculation of Small Molecular Interactions by the Differences of Separate Total Energies. Some Procedures with Reduced Errors. Mol. Phys. 1970, 19, 553–566. Mol Phys 100:63–63
36. Boys SF, Bernardi F (2002) The calculation of small molecular interactions by the differences of separate total energies. Some procedures with reduced errors. Mol Phys 100:65–73
37. Liu B, McLean AD (1973) Accurate calculation of the attractive interaction of two ground state helium atoms. J Chem Phys 59:4557–4558
38. Frisch MJ et al (2009) Gaussian 09. Gaussian, Inc., Wallingford
39. Becke AD (1993) Becke's three parameter hybrid method using the LYP correlation functional. J Chem Phys 98:5648–5652
40. Lee C, Yang W, Parr RG (1988) Development of the Colle-Salvetti correlation-energy formula into a functional of the electron density. Phys Rev B 37:785–789
41. Vosko SH, Wilk L, Nusair M (1980) Accurate spin-dependent electron liquid correlation energies for local spin density calculations: a critical analysis. Can J Phys 58:1200–1211
42. Stephens PJ, Devlin FJ, Chabalowski CF, Frisch MJ (1994) Ab initio calculation of vibrational absorption and circular

dichroism spectra using density functional force fields. J Phys Chem 98:11623–11627
43. McLean AD, Chandler GS (1980) Contracted Gaussian-basis sets for molecular calculations. 1. 2nd row atoms, Z = 11–18. J Chem Phys 72:5639–5648
44. Raghavachari K, Binkley JS, Seeger R, Pople JA (1980) Self-consistent molecular orbital methods. 20. Basis set for correlated wave-functions. J Chem Phys 72:650–654
45. Chai J-D, Head-Gordon M (2008) Long-range corrected hybrid density functionals with damped atom-atom dispersion corrections. Phys Chem Chem Phys 10:6615–6620
46. Dunning TH Jr, Hay PJ (1977) Gaussian basis sets for molecular calculations. In: Schaefer HF (ed) Modern theoretical chemistry, vol 3. Plenum, New York, pp 1–28
47. Wadt WR, Hay PJ (1985) Ab initio effective core potentials for molecular calculations—potentials for main group elements Na to Bi. J Chem Phys 82:284–298
48. Møller C, Plesset MS (1934) Note on an approximation treatment for many-electron systems. Phys Rev 46:618
49. Brauer B, Kesharwani MK, Martin JML (2014) Some observations on counterpoise corrections for explicitly correlated calculations on noncovalent interactions. J Chem Theory Comput 10:3791–3799
50. Reid SA, Nyambo S, Muzangwa L, Uhler B, Π-Stacking (2013) C–H/Π, and halogen bonding interactions in bromobenzene and mixed bromobenzene–benzene clusters. J Phys Chem A 117:13556–13563
51. Tarakeshwar P, Choi HS, Kim KS (2001) Olefinic vs aromatic Π–H interaction: a theoretical investigation of the nature of interaction of first-row hydrides with ethene and benzene. J Am Chem Soc 123:3323–3331
52. Sobczyk L, Grabowski SJ, Krygowski TM (2005) Interrelation between H-bond and Pi-electron delocalization. Chem Rev 105:3513–3560

Affiliations

Madhubabu Alaparthi[1] · Dayton Jonathan Vogel[1] · Andrew G. Sykes[1]

[1] Department of Chemistry, University of South Dakota, Vermillion, SD 57069, USA